Article:
Du, X, Yang, F, Liu, Y et al. (2023) Light-Driven Dynamic Hierarchical Architecture of Three-Dimensional Self-Assembled Cholesteric Liquid Crystal Droplets. Langmuir, 39 (4). pp. 1611-1618. ISSN: 0743-7463

https://doi.org/10.1021/acs.langmuir.2c03040

Light-driven dynamic hierarchical architecture of three-dimensional self-assembled cholesteric liquid crystal droplets

Xiaoxue Du,[1, 2, #] Fei Yang,[1,#] Yanjun Liu,[1] Helen F. Gleeson[2,] and Dan Luo[1,*]*

[1] Department of Electrical and Electronic Engineering, Southern University of Science and Technology, Shenzhen, 518055, China

[2] School of Physics and Astronomy, University of Leeds, Leeds, LS2 9JT, UK

*luod@sustech.edu.cn

*h.f.gleeson@leeds.ac.uk

#These authors contributed equally to this work.

KEYWORDS: cholesteric liquid crystal, droplets, azobenzene liquid crystals, light-driven, topological configuration.

ABSTRACT: Cholesteric liquid crystals have attracted much attention in biosensors, in communication systems, security identification, hierarchical materials assembly, and microlasers, due to their complex and interesting structures accompanied with particular optical properties making them low-cost, label-free and sensitive. However, the reports of CLC droplets with stable topological configurations are still very limited, which hinders the fast development

and broad application of CLC droplet-based devices. In this paper, we manifest light-driven changes in the topological configuration of cholesteric liquid crystals droplets, examined experimentally. Photo-responsive azo-LC doped CLC droplets were manipulated by irradiation by UV light to form novel topological configurations with stable 3D structures. The phenomenon behind the configuration changes is the light-induced cholesteric-isotropic phase transition that takes place in liquid crystals. Several topological configurations of CLC droplets have been demonstrated such as closed-ring structures with cone-shaped centers and concentric elliptical centers, and open-ring structures formed under uni-directional illumination of UV light. Structures with parallel CLC pitch lines at the centre and with a central point singularity are also formed under multi-directional illumination. The competition of the elastic energy and surface energy of the CLC droplets results in the formation of the new topological configurations. All proposed configurations are stable and controllable by light, which enable CLC droplets novel topological structures with new characteristics and provide a lot of potential applications in biosensors and microlasers.

INTRODUCTION

In recent years, cholesteric liquid crystals (CLCs) confined in restricted geometries have been investigated extensively, research driven in part by the popularity of liquid crystal-based smart devices [1-4]. In order to localize the material and be protected from the environment, the majority of applications, for example temperature sensors, expect some form of encapsulation of CLC [5]. The typical form of CLC in restricted geometries is in spherical particles and as such CLC droplets [6-8] exhibit a lot of potential applications in such as environmental sensors and biosensors [9-11], communication system [12-13], security identification [13-14], hierarchical materials assembly [15], and microlasers [12, 16]. CLC droplets have complex and interesting

3D structures accompanying with particular physical and optical properties of low-cost, label-free and sensitive. For this purpose, the application of CLC droplets is highly dependent on their internal structure which determines the optical properties and thus influences the characteristics of the devices. However, the reports CLC droplets with stable topological structures are still very limited, and most of them are restricted to Frank-Pryce structure (onion-like concentric structure with a line defect) [9-10,12-14], which extremely hinders the fast development and broad application of CLC droplets-based devices. The configuration of the liquid crystal droplets is significantly influenced by the intricate three-dimensional winding of produced topological line defects [17-19]. The topological defects and disclination lines with varying winding numbers that cross the liquid crystal layer have an impact on the topology of the fields [18]. Besides, the winding trajectory of the defects induced by chirality in the dynamics should be taken into consideration [19]. We previously tried LC/phospholipid combinations to realize an analyte-induced droplets transition between a Frank–Pryce structure (with planar anchoring) and a nested-cup structure (with perpendicular anchoring), which suggested as a prime option for being used as the foundation for creating inexpensive, single-use sensor devices based on liquid crystal [20]. Therefore, it is highly desirable to explore new strategies for forming stable topological structures in CLC droplets, which will largely broaden the potential application of CLC droplets with novel properties and excellent characteristics.

Several methods have been proposed for tuning the topological structure of CLC droplets both in experiments and simulations [6-7, 21-22]. Frank-Pryce structure, nested-cup structure, equatorial structure, were evidenced in the droplets for several biological applications [20]. The structure of CLC droplets can be regulated by changing the solute in solution [1, 20, 22-23], changing the temperature of a solution [24-26], changing the pitch of the CLC by light [12, 27].

The alteration of a surfactant, for example, sodium dodecyl sulfate [22], imidazolium ionic liquids [23] and phospholipid [20] can control the surface anchoring of droplets, whose structures are relatively stable. The reconfiguration of CLC droplets can be realized by changing the temperature of the solution [24-26]. The droplets will switch from isotropic to a Frank-Pryce structure when cooled down [24]. In addition, the structure in droplets can be influenced through changing the pitch of CLC and surface anchoring by light [12, 27]. Wang et al. evidenced a light-driven chiral switch through the combination of left-handed axially chiral molecular and right-handed photo-insensitive chiral dopant. The droplet's configuration switched from Frank-Pryce to bipolar nematic upon UV light irradiation [12]. Orlova et al. explained that the spiraling structure's pitch gradually increases until it vanishes forming a bipolar configuration [27]. Nevertheless, all the previous methods can only obtain CLC droplets with limited structures of Frank-Pryce or chiral bipolar structure. Electric field [28] and magnetic field [29-30] were applied on the CLC droplets to achieve new topological configurations. According to Swisher's work, the Frank-Pryce structure elongates into a prolate ellipsoid with increasing electric field strength before the director becomes parallel to the field [28]. Mullol et al. reported inducing an elliptical concentric structure using magnetic field [30]. Although electric and magnetic fields can induce the CLC droplets to form new configurations, the fields must be maintained to retain such configurations. Besides, the uniform field induction, as well as the homogeneous molecular interaction we mentioned before, limit the diversity of the new configurations. Therefore, how to achieve new topological configurations in CLC droplets with 3D structures that are stable in the absence of an external stimulus is still a challenge.

In this paper, light-driven topological changes in the configuration of cholesteric liquid crystals droplets have been investigated experimentally. Photo-responsive azobenzene liquid

crystal (azo-LC) doped CLC droplets were manipulated by irradiation using ultraviolet (UV) light to form novel topological configurations with 3D structures that are stable on removal of the illumination. The configurations form as a result of phase transitions in the CLCs. The droplets can remain their new configurations for more than three hours at the room temperature in the presence of fluid disturbance and removal of external stimuli, which can be regarded as relative stable structures. Several topological configurations have been demonstrated under one-directional illumination of UV light such as closed-ring structures with cone-shaped centers and concentric elliptical centers, and open-rings structures. Structures with parallel CLC stripes center and with central point singularity can be formed under multi-directional UV illumination. A wide range of potential applications in biosensors and microlasers are made possible by the fact that all of the proposed configurations of CLC droplets are stable and light controllable.

MATERIALS AND METHODS

A microfluidic chip based on polydimethylsiloxane (PDMS) is used to generate CLC droplets by mixing the CLC mixture (as shown in Table 1) into a buffer that consists of polyvinyl alcohol (PVA), sodium dodecyl sulfate (SDS), and deionized water (DI water). The PVA and SDS is used to ensure a planar and vertical alignment of the LC director at the droplet surface, respectively. These two kinds of surfactants (PVA and SDS) will compete with each other in the alignment process if mixed. The CLC mixture consists of the nematic liquid crystal 5CB (4-Cyano-4'-pentylbiphenyl, purchased from HCCH), the chiral dopant S811 (obtained from HCCH), and the azo-LC 1205 (purchased from Beam.co). Table 1 shows three kinds of CLC mixtures used in our experiments (M1, M2, and M3). For the CLC materials mainly utilized in the following experiments, M2, its nematic-isotropic transition is 34.82 ℃. After

generation, the CLC droplets are transferred onto a glass slide to observe the structure and physical properties using polarization optical microscopy (POM, Nikon Ci).

Table 1. The composition of the CLC mixtures used in the different experiments

	5CB	S811	Azo-LC 1205
M1	95 wt%	1 wt%	4 wt%
M2	94 wt%	2 wt%	4 wt%
M3	93 wt%	3 wt%	4 wt%

The droplets were generated with the microfluidic chip. Fig. 1(a) and 1(b) demonstrate a schematic illustration and microscope image of the microfluidic setup for CLC droplet generation, respectively. To fabricate the microfluidic chip, a photomask was firstly fabricated and then used in a lithographic process to transfer the pattern to SU-8 photoresist on the silicon wafer. The process of graphic transfer generally includes the following steps: pretreatment (wafer clean, pre-bake, primer vapor), photoresist coating, pre-bake, exposure, post-bake, development and hard bake. The elastic PDMS substrate was made by using the molding method after a master chip was made. The basic principle of the molding method is pouring PDMS on the mold with thickness around 1 mm for curing at 75 ˚C for 3 hours. Then the PDMS layer was peeled carefully and put into the plasma cleaner for 1 min. Lastly, the PDMS substrate can be bonded with a glass slide to form a microfluidic chip. The width of the channel on the microfluidic chip is 150 μm. There are two inlets in this droplet formation device, where the buffer is injected from the left entrance as the outer aqueous and divided into two side channels at the first conjunction, as the yellow arrows show. The CLC mixture (M2) is pumped into the chip through the middle entrance and surrounded by the buffer at the second conjunction. CLC droplets with diameter of 60 μm and pitch of 4.9 μm (inset figure) can be generated from the right-hand outlet when the flow rate of CLC mixture and buffer are set to be 0.01 μl/s and 0.25

μl/s, respectively. By changing the flow speed of the buffer and CLC mixture, the size of the generated droplets can be adjusted.

RESULTS AND DISCUSSION

The azo-LC are nematic in their trans-state and can be transformed into the isotropic phase (cis-state) by the stimulation *via* ultraviolet (UV) light [31]. The particular characteristic of this work is the asymmetric introduction of a new interface in the droplets: the isotropic-CLC (iso-CLC) interface. The iso-CLC interface can trigger changes of the internal structures of the CLC droplets and finally results in different metastable topological architectures. Under irradiation with UV light, the part of a CLC droplet on which the UV light is incident quickly transforms into the isotropic phase, while the region away from UV light remains as CLC. The local liquid crystal director of the remaining CLC area in the droplet is affected by the elastic energy and the shape of the iso-CLC interface. The CLC stripes represent the pitch lines, which is parallel to the local liquid crystal director. After turning off the UV light at an appropriate time, the isotropic part of CLC droplet gradually recovers to CLC. During the recovery process, different structures can be obtained in the CLC droplet.

During the phase transformation of photo-controlled cholesteric liquid crystal droplets, it has been found that the interface morphology of the CLC boundary is related to the planar anchoring strength of the droplet's surface [6, 21]. The PVA solution provides CLC droplets with planar surface anchoring while the SDS decreases the strength of planar surface anchoring. The strength of the planar anchoring of liquid crystal molecules on the surface of the droplets can be changed by adjusting the concentration of PVA and SDS [20]. The concentration of PVA is fixed to 3 wt% and the concentration of SDS was set to be 0, 0.1, and 0.2 wt% separately. All of the droplets present a Frank-Pryce structure in the original state. After generating them from the

microfluidic device, the CLC droplets are further illuminated by UV light (365 nm, 1.5 mW/cm^2) in this section of experiment. Using varying concentrations of SDS in buffer allows the CLC droplets to demonstrate different topological structures under the same illumination conditions.

Fig.1(c)-1(e) show three typical states of the CLC droplets after UV light illumination, where the corresponding LC-isotropic phase interface demonstrates different shapes due to different buffers. The strength of surface anchoring plays a significant role in the light phase transition. The transformation area (the black area or isotropic phase) in the CLC droplet is induced by the UV light, where the decrease in order resulting from the trans-cis isomerization of the azo-LC induces a transition from the LC phase to the isotropic phase. In Fig.1 (c), where the buffer contains 3 wt% PVA, 0.2 wt% SDS and deionized water, the UV light induced phase boundary is convex; the isotropic region takes the shape of a crescent moon. The photo image is obtained under POM, where P and A represent the polarizer and analyzer directions respectively. When the concentration of SDS is reduced to 0.1 wt% or 0 wt%, as illustrated in Fig. 1(d) and 1(e), the edge of the UV light induced transformation area varies as well. In our following experiment, to achieve phase transition of CLC droplets more easily at the same UV light intensity, the concentration of PVA and SDS is fixed at 3 wt% and 0.2 wt%, respectively.

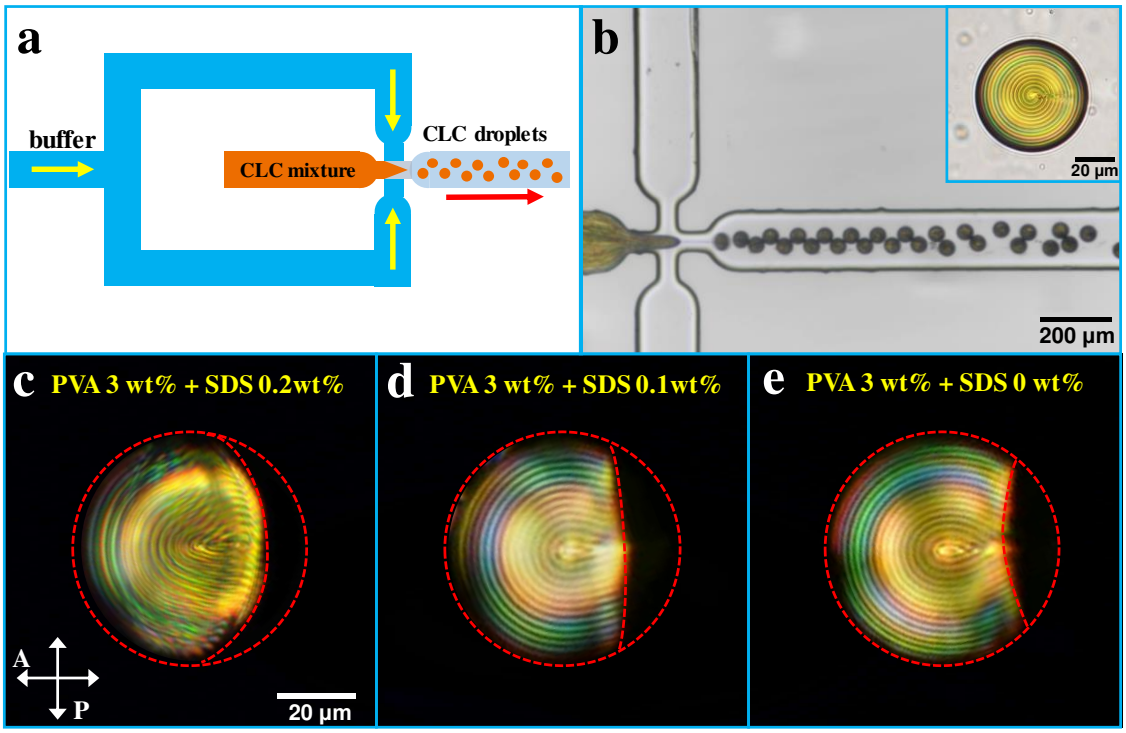

Figure 1. (a) Schematic illustration of microfluidic device. (b) Photograph of the microfluidic device presenting the production of the CLC droplets (using M2). The inset figure shows a brightfield image of a CLC droplet produced in the apparatus with a diameter of 60 μm and pitch of 4.9 μm. Polarizing microscopy images of CLC droplets after UV light illumination (365 nm, 1.5 mW/cm^2) in buffers comprising (c) 3 wt% PVA and 0.2 wt% SDS, (d) 3 wt% PVA and 0.1 wt% SDS. and (e) 3 wt% PVA and 0 wt% SDS. The scale bar is 20 μm in images (c) – (e).

Fig. 2(a) illustrates the experimental setup to observe the CLC droplet using M2 during the UV-induced phase transition. The CLC droplet is dispersed in aqueous solution containing about 3 wt% PVA and 0.2 wt% SDS. The CLC contains 2 wt% S811, 4 wt% 1205 and 94 wt% 5CB. The UV light has a wavelength of 365 nm and an intensity of 5 mW/cm^2. The ideal direction of UV light illumination should be horizontal which helps to observe the progress of the phase transition interface in the CLC droplets. However, UV light that is incident horizontally will be strongly scattered by the glass slide, so the incidence direction is set to be deviated from the

horizontal direction by 30° in our experiment. The schematic structure of initial CLC droplet with the well-defined Frank-Pryce structure is depicted in Fig. 2(b), where the LC, trans-azo-LC, and cis-azo-LC are represented by green rods, brown rods, and a bending rod, respectively. The dynamic process of the light-driven phase transition in CLC droplet observed under POM at 0 s, 24 s, 30 s, and 42 s of UV light exposure, is shown in Fig. 2(c)-2(f), respectively. Before UV light exposure, the CLC droplets is completely cholesteric (Fig. 2(c)). After UV light exposure, the azo-LC molecules will absorb UV light and undergo a transition from the trans-state to the cis-state, which induces an LC-isotropic phase transition. This transition progresses with time, causing the isotropic region to grow (Fig. 2(d)-2(e)). The CLC and isotropic regions can distinguish in POM by their vivid birefringence color and dark appearance, respectively. The azo-LC molecules in their cis-state do not absorb UV light which means the isotropic region in droplet transmits the UV light, thus the UV light will continue to go deep into the droplet until the droplet completely transitions to the isotropic phase (Fig. 2(f)).

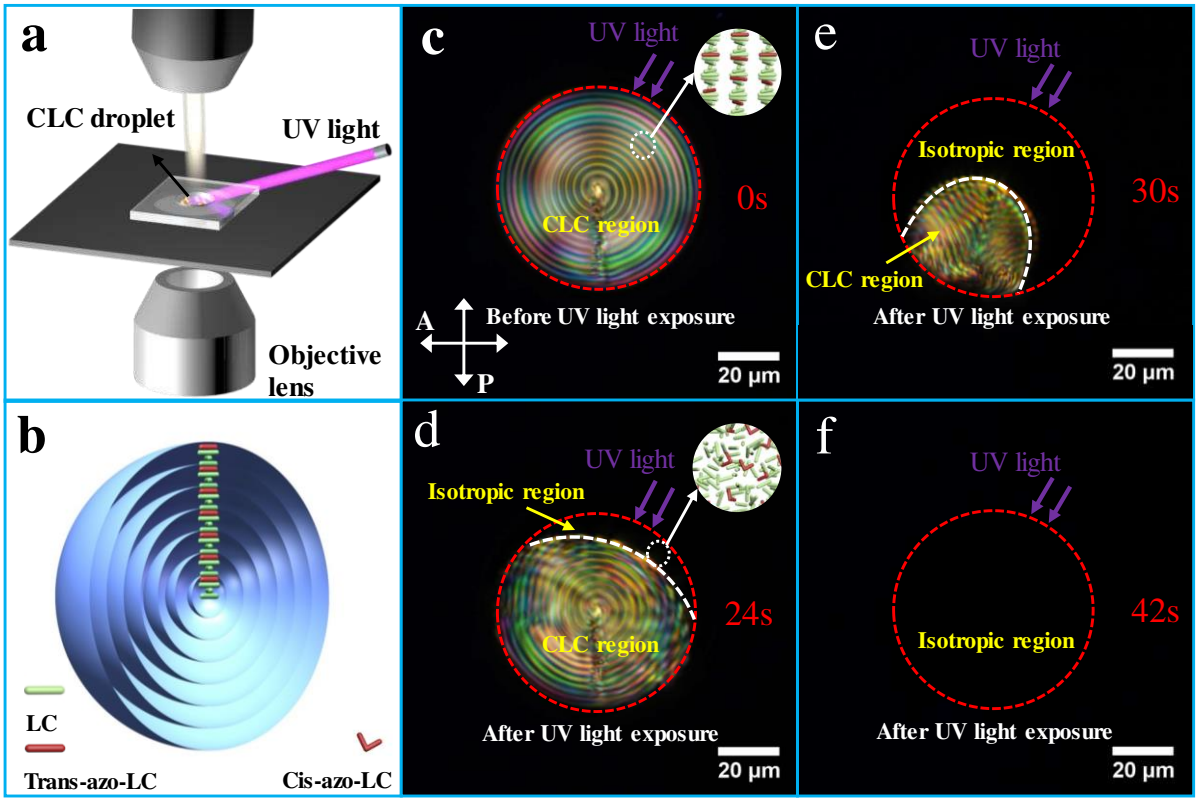

Figure 2. (a) The experimental setup to observe the CLC droplet during the phase transition triggered by UV light. (b) The schematic diagram of the CLC droplets with planar surface alignment – the Frank-Pryce structure. The dynamic process of the light-driven phase transition in the CLC droplet (using M2) observed under POM at (c) 0 s, (d) 24 s, (e) 30 s, and (f) 42 s of UV light exposure. The wavelength of the UV light is 365 nm, and the intensity is 5 mW/cm^2.

The next stage considers how the light driven phase transition can be used to direct the configurations of CLC droplets. The UV light was turned off at specific points during the phase transition and the droplets with a crescent-shaped isotropic region (as in Figure 1(c)) were seen to form new structures. CLC droplets with a Frank-Pryce structure are known to be particularly stable because they not only keep the Frank-Pryce structure during considerable perturbation such as water flow, but also make self-recovery to the initial state even after partial disordering [20]. It is intuitive that the structure of CLC droplet can restore to the Frank-Pryce structure

quickly if the UV light is turned off at a very early stage of phase transition, which was verified in our experiments. If the UV light is turned off extremely early or when the droplet has entirely transitioned to the isotropic phase, the droplet can return to its original Frank-Pryce structure. The key point that determines the relaxed topological structure of the CLC droplet is how much the phase transition trigger CLC droplets to form some new topological structures after turning off the UV light.

A central angle θ that corresponds to the angle between the droplet equator and the edge of the isotropic phase at the surface of the CLC droplet can be used to represent the progress of the light-driven phase transition, as shown in Fig. 3(a). Two forces might trigger the topology change of CLC droplets. The first force $F_{interface}$ is from the iso-CLC interface and exerted on the ends of CLC stripes in contact with the interface which tends to bend CLC stripes to be perpendicular to the interface. The $F_{interface}$ causes a collective motion of the CLC pitch lines along with the interface. The other force $F_{elasticity}$ comes from the elasticity energy. These two forces work together to reorganize the part of CLC stripes to be straight and perpendicular to the interface. The reorganized CLC stripes are dominated by the elasticity energy and the iso-CLC interface energy (called as EI stripes in the following) while the other CLC stripes are still remain as Frank-Pryce structure, as shown in Fig. 3(b).

The value of the threshold θ in CLC droplets determines the distinct topological differences that occur following the cessation of the UV radiation through the recovery of CLC from the isotropic phase. Beyond the threshold, the structure of central CLC pitch lines will be maintained during the broadening of the isotropic phase area, and the shape of the inner CLC stripes is stretched as spherical cones in the recovery even if the UV light is turned off. The threshold θ in CLC droplets is related to the diameter (R) of CLC droplet as shown in Fig. 3(c), where θ

increases as the R increases. The stretching of CLC stripes is mainly induced by the suppressed bending energy of CLC layers. The density of bending energy can be expressed as:

$$E = \frac{1}{2} k_{33} \left(\frac{\partial n_x}{\partial z} + \frac{\partial n_y}{\partial z} \right)^2, \quad (1)$$

where E is the density of bending energy, k_{33} is the bend elastic constant. The small, non-zero components n_x and n_y describe the fluctuations of the optical axis at any point, and z axis is the optical axis [32-34].

The density of the bending energy in Frank-Pryce structure is inversely proportional to r^2 ($E \propto 1/r^2$), where r represents the maximum curvature radius of the CLC stripes in the isotropic region, as reflected in Fig. 3(a). For CLC droplets with a fixed radius R, the curvature radius r of the CLC stripe near the iso-CLC interface decreases with the progress of the isotropic phase boundary and the density of the suppressed bending energy increases. The higher bending energy stretches the inner CLC stripes towards the interface more easily in this situation. The distance r from a droplet's center to the interface increases when the radius R of the droplet increases, even though the central angle θ corresponding to the isotropic phase is a constant. This can explain why a larger CLC droplet requires a larger threshold angle θ to achieve a particular density of bending energy of the CLC stripes near the interface.

Once the angle θ is larger than the threshold in a CLC droplet, the topological structure of CLC stripes will change, driven by the free energy. The distorted stripes store potential energy that hinders a perfect recovery of the Frank-Pryce structure when the UV light is turned off and CLC droplets with new metastable configurations can be obtained. The stretched inner stripes finally become perpendicular to the interface as shown in Fig. 3(b). The relationship between the threshold θ of the isotropic state and the diameter of the droplet during the light-controlled phase transition induced onion-like cholesteric liquid crystal droplets to produce stripes. The trend is

depicted in Fig. 3 (c), which demonstrates that the larger the droplet diameter, the larger the threshold θ.

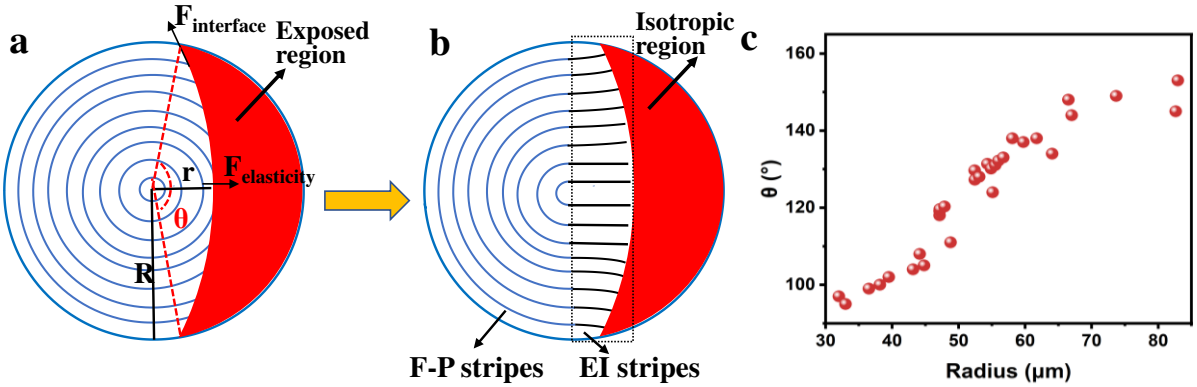

Figure 3. (a) A schematic of a CLC droplet at the initial state and the critical state with a partial phase transition. $F_{interface}$ is the force from iso-CLC interface exerted on the ends of CLC stripes in contact with the interface which tends to bend CLC stripes to be perpendicular to the interface. $F_{elasticity}$ is the force from the elasticity energy. R is the radius of the droplet and r represents the distance between the center and the edge of the exposed region. (b) The schematic of metastable configuration of the CLC droplet. Frank-Pryce (F-P) stripes show a concentric circular configuration. EI stripes form in the reconfiguration area, induced by competition between the elasticity energy and iso-CLC interface energy. (c) The threshold θ in CLC droplets versus the diameter (R) of CLC droplet.

Fig. 4 (a) depicts the formation process of a topological structure with a cone-shaped center within the CLC droplets (using M1) triggered by the phase transition under UV light. The UV exposed region, which initially becomes isotropic, is represented by the green and dark region in Fig. 4(a)-i (schematic illustration) and Fig. 4(a)-ii (photo image under POM), respectively. The initial structure of the CLC droplet is Frank-Pryce, which can be regarded as closed circular stripes and the existence of the isotropic phase breaks the integrity of the stripes that are in contact with the phase interface. After turning off the UV light, the isotropic phase will gradually

transition to the CLC phase while the shapes of the inner CLC stripes change. The final recovered structure is shown in Fig. 4(a)-iii (schematic illustration) and Fig. 4(a)-iv (photo image under POM), respectively. It can be seen that the final inner CLC stripes formed from the isotropic region are cone shaped. The shape change mainly comes from the elasticity energy. The existence of the isotropic phase frees the suppressed elasticity energy especially the bending energy, which is resulted from the competition of elasticity energy and surface energy. The force $F_{elasticity}$ stretches the central circular stripes towards the iso-CLC interface.

With more UV light illumination, the area of the isotropic region formed increases accordingly, resulting in several different topological structures that can occur after removing the UV light. Fig. 4(b) demonstrates a topological structure with concentric ellipses, where the formed CLC stripes look similar to running tracks. When the UV light exposure time increases further, two open ring structures can be formed accompanied with non-recovery of the isotropic region in final meta-stable state, as illustrated in Fig. 4(c) and Fig. 4(d). The exposure region (Fig. 4(c)-i, ii) is controlled to a threshold value to make the EI stripes parallel to the iso-CLC interface after recovery (Fig. 4(c)-iii,iv), resulting in an open ring structure of CLC droplet. When the UV illumination further increases to form a concave shape of CLC region (Fig. 4(d)-i,ii), which induces EI stripes to be divergent. Potential energy is stored in those divergent EI stripes and this promotes the later growth of CLC stripes that keep the divergent orientation. However, the divergent orientation is not preferred by the surface anchoring. After turning off the UV light, the shaping effect of surface energy increases and the CLC stripes become as smooth as possible. Owing to the shifting away of the interface, there will be an increase of Frank-Pryce structure stripes and the elimination of the distinct transition between Frank-Pryce structure stripes and EI stripes. The divergent orientation of CLC stripes can be quickly

destroyed by surface energy and replaced by the parallel stripes if the potential energy of the divergent orientation is not sufficient. The divergent orientation of stripes can be kept only if the potential energy is strong enough to compete with surface anchoring, leaving a divergent orientation with acute angle structure in in the recovered topology (Fig. 4(d)-iii,v). It is noticed that a similar topological structure of CLC droplet also can be formed by M3 with higher chirality and smaller pitch, as illustrated in Fig. 4(a)-v to Fig. 4(d)-v.

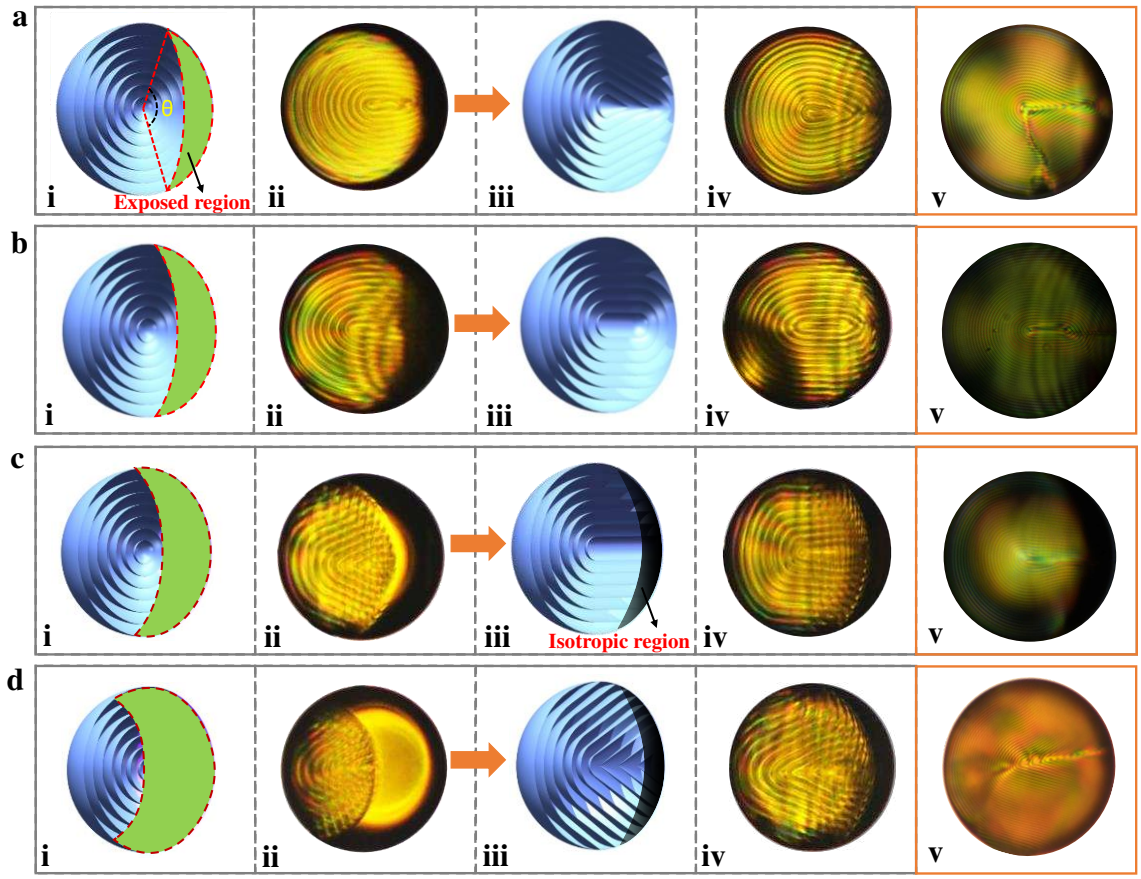

Figure 4. The formation process of a topological structure with cone-shaped center of CLC droplets triggered by the phase transition under UV light. The exposure time and therefore the isotropic region are gradually increased, resulting in topological structure of (a) cone-shaped, (b) concentric ellipses-shaped, (c) open ring-shape with parallel EI stripes, and (d) acute angle-shape. (i) the 3D schematic illustrations of phase transition region in CLC droplet; (ii) the photo

images of the CLC droplet under POM corresponding to (i); (iii) the 3D schematic figure of the final recovered structure of CLC droplet after turning off UV light; (iv) the photo images of the droplet under POM with a lower chirality (M1) corresponding to (iii); (vi) the photo images of the droplet under POM with a higher chirality (M3) corresponding to (iii).

Besides illuminating CLC droplets in one direction, new topological structures of CLC droplets can also be formed by UV exposure from two directions. The bi-directional exposure can be carried either simultaneously or sequentially. In our experiments, the two UV exposures are applied sequentially on the CLC droplet. Fig. 5(a) and Fig. 5(b) shows schematic illustrations and experimentally obtained photo images of the bi-directional exposure, respectively. The CLC droplet is first exposed to UV light from one side to produce an iso-CLC interface before the droplet center, which stretches CLC stripes towards the interface (Fig. 5(a & b)-i). After turning off the UV light, parallel CLC stripes are formed in the exposure area (Fig. 5(a & b)-ii). The parallel stripes are quite stable because the surface anchoring is not strong enough to surmount the repulsion from the merge of CLC stripes. Then the same exposure but from the opposite direction (Fig. 5(a & b)-iii) is applied to the CLC droplet to induce parallel stripes from Frank-Pryce stripes (Fig. 5(a & b)-iv). It is noticed that a similar topological structure of CLC droplet also can be formed by M3 with higher chirality and smaller pitch, as shown in Fig. 5(a)-v and Fig. 5(b)-v.

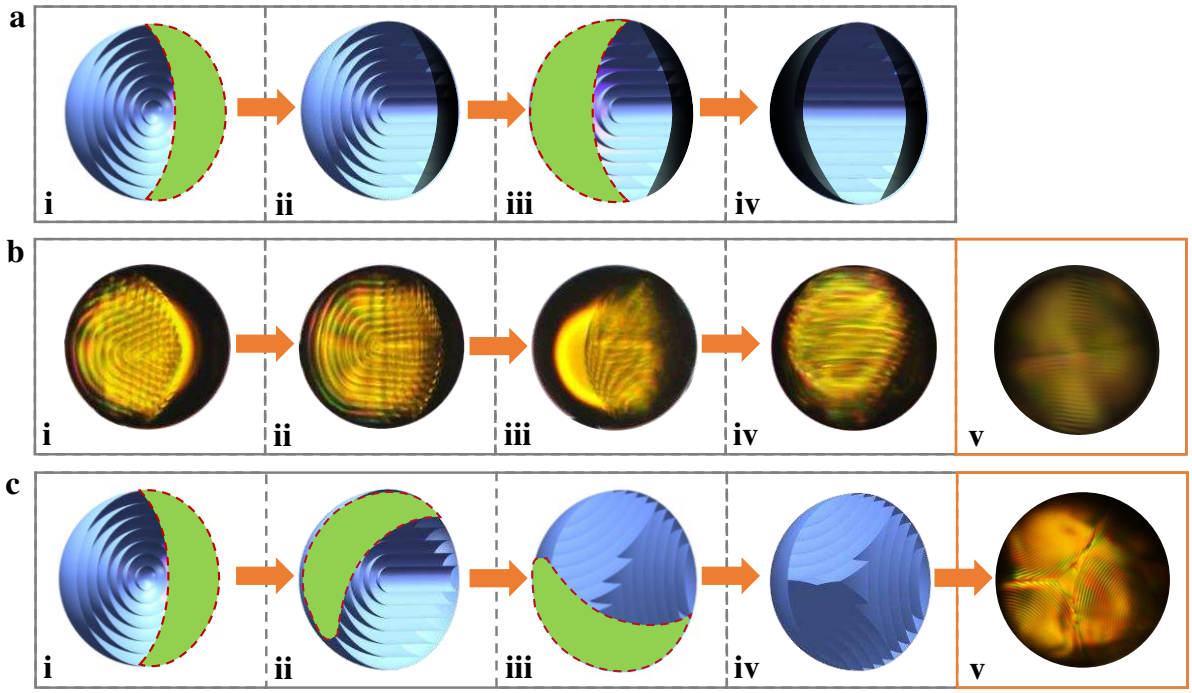

Figure 5. (a) Schematic illustration of bi-directional exposure of the CLC droplets. (b) POM photo images of two-directional exposure of CLC droplets. (i) the first UV exposure; (ii) recovered structure after the first exposure; (iii) the second UV exposure; (iv) the recovered structure after the second exposure (using M1); (v) the recovered structure after a second exposure on M3. (c) Tri-directional exposure of CLC droplets (using M3). (i)-(iii) schematic illustration of the first to the third UV exposures; (iv) schematic illustration of the structure recovered after the tri-directional exposure. (v) POM photo image of the recovered structure after the tri-directional exposure.

Tri-directional exposure with a 120^{o} angle between the three exposures in the same plane induced CLC droplets (using M3) also shows another new topological structure, Fig. 5(c). The schematic illustration of transformation process is shown in Fig. 5(c) i-iv, where three exposures of UV light are employed step by step on a CLC droplet, leading to a hyperbolic triangle structure with central point singularity and three-fold symmetry [Fig. 5(c)-v].

CONCLUSION

In this study, we have demonstrated a wide variety of new, light-driven topological configurations to occur in cholesteric liquid crystals droplets experimentally. Photo-responsive azo-LC doped CLC droplets were manipulated by irradiation of UV light to form novel topological configuration of CLC droplets with stable 3D structure through phase transition of liquid crystals. Several topological configurations of CLC droplets have been demonstrated such as closed-ring structures of cone-shaped center and concentric ellipses center, and open-ring structures under uni-directional illumination of UV light, as well as structures with parallel CLC stripes center and with central point singularity under multi-directional illumination of UV light. The competition of the elastic energy and surface energy of CLC droplets leads to the formation of the new topological configurations. All of the CLC droplet configurations that have been suggested are stable and light-controllable, allowing for novel topological structures with novel properties and a wide range of possible applications in biosensors and microlasers.

ACKNOWLEDGEMENTS

This work is supported by the National Natural Science Foundation of China (NSFC) (62175098 and 61875081), and Guangdong Basic and Applied Basic Research Foundation (2021B1515020097).

REFERENCES AND LINKS

(1) Tran, L.; Lavrentovich, M. O.; Durey, G.; Darmon, A.; Haase, M. F.; Li, N.; Lee, D.; Stebe, K. J.; Kamien, R. D.; Lopez-Leon, T. Change in Stripes for Cholesteric Shells Via Anchoring in Moderation. *Phys. Rev. X* **2017**, *7*, 041029.

(2) Chen, J.; Lacaze, E.; Brasselet, E.; Harutyunyan, S. R.; Katsonis, N.; Feringa, B. L. Textures of Cholesteric Droplets Controlled by Photo-Switching Chirality at The Molecular Level. *J. Mater. Chem. C* **2014**, *2*, 8137–8141.

(3) Darmon, A.; Benzaquen, M.; Seč, D.; Čopar, S.; Dauchot, O.; Lopez-Leon, T. Waltzing Route Toward Double-Helix Formation in Cholesteric Shells. *Proc. Natl. Acad. Sci. USA* **2016**, *113*, 9469–9474.

(4) Oswald, P.; Pieranski, P. Nematic and Cholesteric Liquid Crystals. CRC Press, Boca Raton, **2005**, *6*, 384-395.

(5) Demus, D.; Goodby, J.; Gray, G. W.; Spiess, H.-W.; Vill, V. Handbook of Liquid Crystals. Wiley-VCH Verlag Gmbh, Weinheim **1998**, *1 IX.3*, 823-838.

(6) Xu, F.; Crooker, P. P. Chiral Nematic Droplets with Parallel Surface Anchoring. *Phys. Rev. E* **1997**, *56*, 6853–6860.

(7) Bezić, J.; Žumer, S. Structures of The Cholesteric Liquid Crystal Droplets with Parallel Surface Anchoring. *Liq. Cryst.* **1992**, *11*, 593–619.

(8) Tran, L.; Kim, H.-N.; Li, N.; Yang, S.; Stebe, K. J.; Kamien, R. D.; Haase, M. F. Shaping Nanoparticle Fingerprints at The Interface of Cholesteric Droplets. *Sci. Adv.* **2018**, *4*, eaat8597.

(9) Lee, H.-G.; Munir, S.; Park, S.-Y. Cholesteric Liquid Crystal Droplets for Biosensors. *ACS Appl. Mater. Inter.* **2016**, *8*, 26407–26417.

(10) Franklin, D.; Ueltschi, T.; Carlini, A.; Yao, S.; Reeder, J.; Richards, B.; Duyne, R. P. V.; Rogers, J. Bioresorbable Microdroplet Lasers as Injectable Systems for Transient Thermal Sensing and Modulation. *ACS Nano* **2021**, *15*, 2327-2339.

(11) Dubtsov, A. V.; Pasechnik, S. V.; Shmeliova, D. V.; Kralj, S. Light and Phospholipid Driven Structural Transitions in Nematic Microdroplets. *Appl. Phys. Lett.* **2014**, *105*, 151606.

(12) Wang, L.; Chen, D.; Gutierrez-Cuevas, K. G.; Bisoyi, H. K.; Fan, J.; Zola, R. S.; Li, G.; Urbas, A. M.; Bunning, T. J.; Weitz, D. A.; Li, Q. Optically Reconfigurable Chiral Microspheres of Self-Organized Helical Superstructures with Handedness Inversion. *Mater. Horiz.* **2017**, *4*, 1190–1195.

(13) Noh, J.; Liang, H.-L.; Drevensek-Olenik, I.; Lagerwall, J. P. F. Tuneable Multicoloured Patterns from Photonic Cross-Communication Between Cholesteric Liquid Crystal Droplets. *J. Mater. Chem. C* **2014**, *2*, 806–810.

(14) Seo, H. J.; Lee, S. S.; Noh, J.; Ka, J.-W.; Won, J. C.; Park, C.; Kim, S.-H.; Kim, Y. H. Robust Photonic Microparticles Comprising Cholesteric Liquid Crystals for Anti-Forgery Materials. *J. Mater. Chem. C* **2017**, *5*, 7567–7573.

(15) Rahimi, M.; Roberts, T. F.; Armas-Pérez, J. C.; Wang, X.; Bukusoglu, E.; Abbott, N. L.; Pablo, J. J. Nanoparticle Self-Assembly at The Interface Of Liquid Crystal Droplets. *Proc. Natl. Acad. Sci. USA* **2015**, *112*, 5297–5302.

(16) Cipparrone, G.; Mazzulla, A.; Pane, A.; Hernandez, R. J.; Bartolino, R. Chiral Self-Assembled Solid Microspheres: A Novel Multifunctional Microphotonic Device. *Adv. Mater.* **2011**, *23*, 5773–5778.

(17) Senyuk, B.; Pandey, M. B.; Liu, Q.; Tasinkevych, M.; Smalyukh, I. I. Colloidal Spirals in Nematic Liquid Crystals. *Soft Matter* **2015**, *11*, 8758-8767.

(18) Mur, U.; Ravnik, M. Numerical Modeling of Optical Modes in Topological Soft Matter. *Opt. Express* **2022**, *30*, 14393-14407.

(19) Darmon, A.; Benzaquen, M.; Seč, D.; Čopar, S.; Dauchot, O.; Lopez-Leon, T. Waltzing Route Toward Double-Helix Formation in Cholesteric Shells. *PNAS* **2016**, *113*, 9469-9474.

(20) Paterson, D. A.; Du, X. X.; Bao, P.; Parry, A. A.; Peyman, S. A.; Sandoe, J. A. T.; Evans, S. D.; Luo, D.; Bushby, R. J.; Jones, J. C.; Gleeson, H. F. Chiral Nematic Liquid Crystal Droplets as A Basis for Sensor Systems, *Mol. Syst. Des. Eng.* **2022**, *7*, 607-621.

(21) Zhou, Y.; Bukusoglu, E.; Martínez-González, J. A.; Rahimi, M.; Roberts, T. F.; Zhang, R.; Wang, X.; Abbott, N. L.; Pablo, J. J. Structural Transitions in Cholesteric Liquid Crystal Droplets. *ACS Nano* **2016**, *10*, 6484–6490.

(22) Shechter, J.; Atzin, N.; Mozaffari, A.; Zhang, R.; Ross, J. L. Direct Observation of Liquid Crystal Droplet Configurational Transitions Using Optical Tweezers. *Langmuir* **2020**, *36*, 7074-7082.

(23) Ramou, E.; Rebordao, G.; Palma, S. I. C. J.; Roque, A. C. A. Stable and Oriented Liquid Crystal Droplets Stabilized by Imidazolium Ionic Liquids. *Molecules* **2021**, *26*, 6044.

(24) Kolacz, J.; Wei, Q. H. Self-Localized Liquid Crystal Micro-Droplet Arrays on Chemically Patterned Surfaces. *Crystals* **2022**, *12*, 13.

(25) Durey, G.; Ishii, Y.; Lopez-Leon, T. Temperature-Driven Anchoring Transitions at Liquid Crystal / Water Interfaces. *Langmuir* **2020**, *36*, 9368-9376.

(26) Yoshioka, J.; Araoka, F. Topology-Dependent Self-Structure Mediation and Efficient Energy Conversion in Heat-Flux-Driven Rotors of Cholesteric Droplets. *Nat. Commun.* **2018**, *9*, 432.

(27) Orlova, T.; Aßhoff, S. J.; Yamaguchi, T.; Katsonis, N.; Brasselet, E. Creation and Manipulation of Topological States in Chiral Nematic Microspheres. *Nat. Commun.* **2015**, *6*, 7603.

(28) Swisher, R. R. The Cholesteric-Nematic Transition in Droplets Subjected to Electric Fields. *Liq. Cryst.* **1999**, *26*, 57–62.

(29) Parshin, A. M. Structural Stability of Nematic Liquid Crystal Droplets in The Light of the Catastrophe Theory. *Mod. Phys. Lett. B* **2019**, *33*, 1950434.

(30) Ignés-Mullol, J.; Mora, M.; Martínez-Prat, B.; Vélez-Cerón, I.; Herrera, R. S.; Sagués, F. Stable and Metastable Patterns in Chromonic Nematic Liquid Crystal Droplets Forced with Static and Dynamic Magnetic Fields. *Crystals*, **2020**, *10*, 138.

(31) Hrozhyk, U. A.; Serak, S. V.; Tabiryan, N. V.; Bunning, T. J. Photoinduced Isotropic State of Cholesteric Liquid Crystals: Novel Dynamic Photonic Materials. *Adv. Mater.* **2007**, *19*, 3244–3247.

(32) Gennes, P. G. Polymeric Liquid Crystals: Frank Elasticity and Light Scattering. *Mol. Cryst. Liq. Cryst.* **1997**, *34*, 177-182.

(33) Landau, L. D.; Lifshitz, E. M. Theory of Elasticity. Pergamon Press, Oxford, **1986**, *7*, 144-145.

(34) Gennes, P. G.; Prost, J. The Physics of Liquid Crystals. Clarendon Press, Oxford, **1993**, *23*, 100-143.

Table of Contents

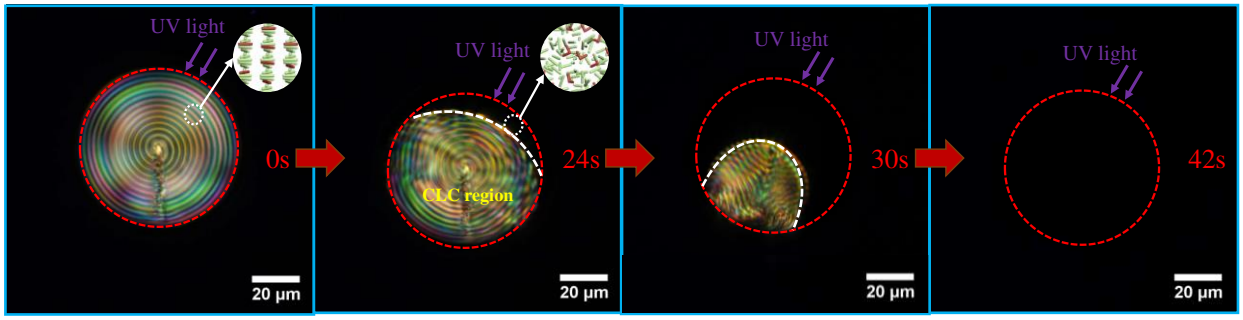

Figure. The dynamic process of the light-driven phase transition in the CLC droplet observed under POM